Nucleon-Nucleon Scattering from One-Boson-Exchange Potentials*

RONALD A. BRYAN†

Laboratoire de Physique Nucléaire, Orsay (Seine et Oise), France

AND

BRUCE L. SCOTT

Department of Physics, University of Southern California, Los Angeles, California

(Received 2 March 1964)

Nucleon-nucleon scattering is studied for laboratory scattering energies over the 0 to 320-MeV range for states with angular momentum $l \geq 1$. Our central hypothesis is that the interaction may be represented by a series of one-boson-exchange potentials. To this end, we attempt to fit the phenomenological models of Lassila *et al.* (Yale) and of Hamada and Johnston with the series of one-boson-exchange potentials due to the ρ, ω, π, and η, with the meson-nucleon coupling constants taken as adjustable parameters. We find that additional attraction is required in the central potentials, and we provide this by introducing two scalar mesons of isotopic spin 0 to 1, respectively. We next consider the nucleon-nucleon phase shifts that have been determined through phase-shift analysis of the N-N data by several groups. We achieve reasonable fits to the P, D, and F states with the following searched parameters: $g_\eta{}^2 = 7.0$, $g_\pi{}^2 = 11.7$, $g_\omega{}^2 = 21.5$, $g_\rho{}^2 = 0.68$, $f_\rho/g_\rho = 1.8$, $m_0 = 560$ MeV, $g_0{}^2 = 9.4$, $m_1 = 770$ MeV, and $g_1{}^2 = 6.5$; the parameters of the $T = 0$ and $T = 1$ scalar mesons are identified by the subscripts 0 and 1, respectively, and

$$\mathcal{L}_{\text{int}}{}^{(P)} = (4\pi)^{1/2} g_\rho \bar{\psi} \boldsymbol{\tau} \gamma^\mu \psi \boldsymbol{\varrho}_\mu + (4\pi)^{1/2} (f_\rho/2m_\rho) \bar{\psi} \boldsymbol{\tau} \sigma^{\mu\nu} \psi [\partial_\nu \boldsymbol{\varrho}_\mu - \partial_\mu \boldsymbol{\varrho}_\nu].$$

Predetermined parameters are $m_\rho = 760$ MeV, $m_\omega = 782$ MeV, $m_\pi = 138.2$ MeV, $m_\eta = 548$ MeV, and $f_\omega/g_\omega = 0$. Because of the r^{-3} behavior of the potentials at the origin, all potentials are set to zero within 0.6 F. This has (surprisingly) little effect in most states but does eliminate bound $^3P_2$ and $^3F_4$ states. The effect of including the ϕ and the relation to other experiments is discussed.

I. INTRODUCTION

THIS is the second in a series of articles treating the low-energy nucleon-nucleon interaction in terms of the new mesons or multipion resonances. The assumption is that the N-N scattering amplitude is mainly given by the one-boson-exchange terms, or poles, of the new mesons. Unitary is introduced by treating the Fourier transform of each Born term as a potential (the so-called one-boson-exchange potential) and inserting the sum of these potentials in the Schrödinger equation. The resulting amplitudes resemble the Born predictions, with the unitarity correction becoming smaller with increasing angular momentum.

In the first article of this series[1] (let us designate it I) we treated the p-p interaction in terms of an effective vector meson (ω-ρ), a scalar meson ($T = 0$, $J = 0^+$) and the pion. The results were sufficiently encouraging to motivate this present analysis of the combined p-p and n-p problem. Other authors have also investigated N-N scattering in terms of one-boson-exchange potentials (OBEP), particularly McKean,[2] Lichtenberg,[3] Hoshizaki, Otsuki, Watari, and Yonezawa,[4] and Babikov.[5] Ramsay[6] has studied the p-p interaction in high-angular-momentum states in terms of just the pole

contributions of the mesons in I. Sawada, Ueda, Watari, and Yonezawa[7] have considered the same (effective) mesons and extended the p-p fits down to P waves, using the K matrix to generate unitarity.

Another school has employed similar Born terms but used dispersion relations in generating unitarity. Such an approach embodies essentially the same physics as the potential approach. Important contributions in this regard have been made by Scotti and Wong.[8] Riazuddin and Moravcsik,[9] and Kantor[10] have also contributed to this approach.

In the work which follows, we shall investigate the N-N interaction by first fitting certain phenomenological N-N potentials with an appropriate sum of one-boson-exchange potentials. After that we shall fit the actual nucleon-nucleon phase shifts. It is advantageous to first fit the potentials because they constitute a much more simple problem and it is possible to understand the role of each meson. The potentials are cast in the form

$$V = V^{(0)} + \boldsymbol{\tau}_1 \cdot \boldsymbol{\tau}_2 V^{(1)}.$$

This decouples the contribution of the $T = 0$ and the $T = 1$ mesons as these may contribute only to $V^{(0)}$ and $V^{(1)}$, respectively. The potentials $V^{(i)}$ are further broken down into the form

$$V^{(i)}(r) = V_C{}^{(i)}(r) \cdot 1 + V_{\sigma\sigma}{}^{(i)}(r) \sigma_1 \cdot \sigma_2$$
$$+ V_T{}^{(i)}(r) S_{12} + V_{LS}{}^{(i)}(r) L \cdot S.$$

[1] R. A. Bryan, C. R. Dismukes, and W. Ramsay, Nucl. Phys. 45, 353 (1963).
[2] R. S. McKean, Jr., Phys. Rev. 125, 1399 (1962).
[3] D. B. Lichtenberg, Nuovo Cimento 25, 1106 (1962).
[4] N. Hoshizaki, S. Otsuki, W. Watari, and M. Yonezawa, Progr. Theoret. Phys. (Kyoto) 27, 1199 (1962).
[5] V. V. Babikov, Progr. Theoret. Phys. (Kyoto) 29, 712 (1963).
[6] W. Ramsay, Phys. Rev. 130, 1552 (1963).
[7] S. Sawada, T. Ueda, W. Watari, and M. Yonezawa, Progr. Theoret. Phys. (Kyoto) 28, 991 (1962).
[8] A. Scotti and D. Y. Wong, Phys. Rev. Letters 10, 142 (1963), and (to be published).
[9] Riazuddin and M. J. Moravcsik, Phys. Letters 4, 243 (1963).
[10] P. B. Kantor, Phys. Rev. Letters 12, 52 (1964).

In principle, there should be a fifth term (quadratic spin-orbit), but it is neglected here because the one-boson-exchange potentials do not have such a term in the nonrelativistic approximation employed here. Fortunately, it is still possible to fit the data (excluding S waves).

The most interesting feature to emerge from this study is the dynamics of the several contributing mesons. The pion, of course, provides the long-range force. The ω provides the "hard core" and short-range spin-orbit attraction in $V^{(0)}$ as accurately predicted by Nambu,[11] Fujii,[12] Breit,[13] Sakurai,[14,15] and others. A $T=0$, $J=0^+$ meson—with the quantum numbers of the ABC particle—is introduced to provide the inter-mediate-range attraction necessary for nuclear binding as well as phase shift fits. The ρ meson shows up most clearly in the cancellation of the pion contribution to $V_T^{(1)}$ at short distances; the ρ's spin-orbit and spin-spin effects are less pronounced but still important in fitting the data.

One other meson is postulated, with quantum numbers $T=1$, $J=0^+$. It is introduced to provide an attraction observed in the phenomenological form of $V_C^{(1)}$ just as the $T=0$, $J=0^+$ meson is introduced to provide the attraction in $V_C^{(0)}$. The final meson considered is the η, whose principle importance is found to lie in the cancellation of the tensor contribution of the ω.

There result in all six mesons, three with isospin 1 and three with isospin 0. Each set of three is comprised of a pseudoscalar, a scalar, and a vector meson. To fit the phenomenological potentials the meson-nucleon coupling constant of each of the mesons is adjusted; also adjusted is the mass of each scalar meson.

After the empirical potentials are matched we attempt to fit the experimentally determined phase shifts. These phases are fit over the 0- to 320-MeV laboratory-scattering energy range. Only P, D, and F phases are fit. The two S states are not investigated here as these are subject to extreme short-range effects and should probably be fit with two additional phenomenological parameters each (corresponding to the scattering length and effective range) after the pole parameters have been determined by the higher partial waves. G waves and higher are also not fit, but for a different reason: Their experimental determination beyond the pion pole contribution is vague. However, these waves are taken into account in the sense that g_π^2 is required to fall in the range determined by the higher partials through Moravcsik-type analysis[16] of N-N data.

[11] Y. Nambu, Phys. Rev. 106, 1366 (1957).
[12] Y. Fujii, Progr. Theoret. Phys. (Kyoto) 21, 232 (1959).
[13] G. Breit, Proc. Natl. Acad. Sci., U.S. 46, 746 (1960); Phys. Rev. 120, 287 (1960).
[14] J. J. Sakurai, Phys. Rev. 119, 1784 (1960).
[15] J. J. Sakurai, Ann. Phys. (N.Y.) 11, 1 (1960).
[16] P. Cziffra, M. H. MacGregor, M. J. Moravcsik, and H. P. Stapp, Phys. Rev. 114, 880 (1959).

II. THE ONE-BOSON-EXCHANGE POTENTIALS

For the convenience of the reader we repeat the formulas for the one-boson-exchange potentials which were given in I. Derivations of these potentials may be found, for example, in the paper by Hoshizaki, Lin, and Machida.[17]

For a $T=0$, $J=0^+$ meson (S), the interaction Lagrangian is given by

$$\mathcal{L}_{int}= (4\pi)^{1/2}g_S\bar{\psi}\psi\phi^{(S)}$$

and the nonrelativistic one-boson-exchange potential is

$$V^{(S)}(r) = g_S^2\left[-\left(1-\frac{1}{8}\frac{m_S^2}{M^2}\right)\Phi(m_S r) \right.$$
$$\left. +\frac{1}{2}\frac{m_S^2}{M^2}\left(1-\frac{1}{8}\frac{m_S^2}{M^2}\right)J(m_S r)\mathbf{L}\cdot\mathbf{S} \right]m_S c^2.$$

Here $m_S=$ scalar meson mass, $M=$ nucleon mass, and $\hbar=c=1$;

$$\Phi(x)=e^{-x}/x$$

and

$$J(x)=(1/x)(d/dx)\Phi(x).$$

For a $T=0$, $J=0^-$ meson (PS), the interaction Lagrangian is taken to be

$$\mathcal{L}_{int}= (4\pi)^{1/2}g_{PS}\bar{\psi}\gamma_5\psi\phi^{(PS)},$$

and the one-boson-exchange potential in the non-relativistic limit becomes

$$V^{(PS)}(r)= g_{PS}^2[\tfrac{1}{12}(m_{PS}^2/M^2)\Phi(m_{PS}r)\boldsymbol{\sigma}_1\cdot\boldsymbol{\sigma}_2$$
$$+\tfrac{1}{4}(m_{PS}^2/M^2)\chi(m_{PS}r)S_{12}]m_{PS}c^2.$$

Here $m_{PS}=$ pseudoscalar meson mass, and

$$\chi(x)= (\tfrac{1}{3}+1/x+1/x^2)\Phi(x).$$

The tensor and spin-orbit operators have the usual meaning

$$S_{12}=3(\boldsymbol{\sigma}_1\cdot\hat{r})(\boldsymbol{\sigma}_2\cdot\hat{r})-\boldsymbol{\sigma}_1\cdot\boldsymbol{\sigma}_2; \quad \mathbf{L}\cdot\mathbf{S}=\tfrac{1}{2}\mathbf{L}\cdot(\boldsymbol{\sigma}_1+\boldsymbol{\sigma}_2).$$

$\boldsymbol{\sigma}_1$ and $\boldsymbol{\sigma}_2$ are the Pauli spin matrices for nucleons 1 and 2; L is the relative angular momentum operator in the center-of-mass system; $\mathbf{r}$ is the interaction separation distance, with magnitude r and direction $\hat{r}$.

For a $T=0$, $J=1^-$ meson (V) the interaction Lagrangian takes the general form

$$\mathcal{L}_{int}= (4\pi)^{1/2}g_V\bar{\psi}\gamma^\mu\psi\phi_\mu^{(V)}$$
$$+ (4\pi)^{1/2}(f_V/2m_V)\bar{\psi}\sigma^{\mu\nu}\psi[\partial_\nu\phi_\mu^{(V)}-\partial_\mu\phi_\nu^{(V)}],$$

with $\sigma^{\mu\nu}$ and the γ matrices defined as in Schweber, Bethe, and de Hoffmann.[18] For convenience, in the analysis to follow, we cast the corresponding one-boson-

[17] N. Hoshizaki, I. Lin, and S. Machida, Progr. Theoret. Phys. (Kyoto) 26, 680 (1961).
[18] S. S. Schweber, H. A. Bethe, and F. de Hoffmann, Mesons and Fields (Row, Peterson, and Company, Evanston, Illinois, 1956), Vol. I.
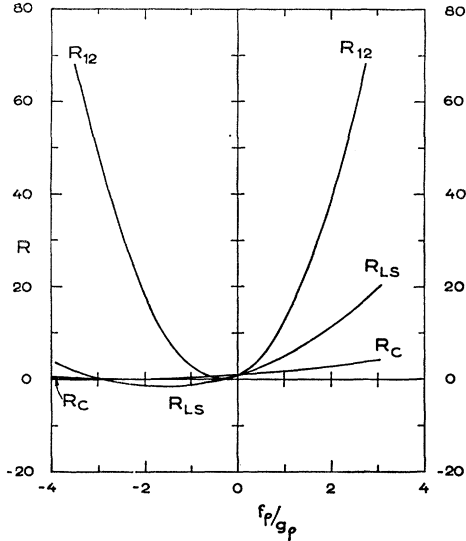
Fig. 1. R_C, R_{LS}, and R_{12} plotted as functions of the ratio of derivative to direct vector meson-nucleon coupling constants.

exchange potential into a form corresponding to just "electric" coupling for the vector mesons, modified by factors due to "magnetic" coupling.

$$V^{(V)}(r)=g_V{}^2\left\{R_C(f_V/g_V)\left(1+\frac{1}{4}\frac{m_V{}^2}{M^2}\right)^2\Phi(m_Vr)\right.$$

$$+R_{12}(f_V/g_V)\frac{1}{4}\frac{m_V{}^2}{M^2}[\tfrac{2}{3}\Phi(m_Vr)\sigma_1\cdot\sigma_2-\chi(m_Vr)S_{12}]$$

$$\left.+R_{LS}(f_V/g_V)\frac{3}{2}\frac{m_V{}^2}{M^2}J(m_Vr)\mathbf{L}\cdot\mathbf{S}\right\}m_Vc^2,$$

where

$$R_C(f_V/g_V)=\left[1+\frac{\frac{1}{2}(m_V/M)f_V}{1+\frac{1}{4}(m_V/M)^2g_V}\right]^2,$$

$$R_{12}(f_V/g_V)=\left[1+\frac{1+\frac{1}{8}(m_V/M)^2f_V}{\frac{1}{2}(m_V/M)g_V}\right]^2,$$

$$R_{LS}(f_V/g_V)=1+\frac{4(m_V/M)f_V}{\frac{3}{2}(m_V/M)^2g_V}+\frac{f_V{}^2}{g_V{}^2},$$

$m_V=$ vector meson mass. It is apparent that each function R converges to unity as $f_V/g_V\rightarrow0$, as it must. These functions are displayed in Fig. 1. The formulas for the vector meson OBEP are correct through order $(m_V/M)^2$.

In order to estimate the error incurred in taking the nonrelativistic approximation, we have calculated the phase shifts in Born approximation as given by (a) the NR potentials above, and (b) the exact pole contributions.[19] At 150 MeV we find that the $J=0^-$ and $J=0^+$

NR Born values are systematically 4% higher than the relativistic (i.e., exact) Born values; that the $J=1^-$ NR Born values do not err systematically, but are on the average 6% in error in absolute magnitude for $f_V/g_V=0$, and 13% in error for $f_V/g_V=2$. The NR error at 300 MeV may be expected to be twice as great.

To determine the one-boson-exchange potentials for $T=1$ mesons, where in the meson field operator ϕ is replaced by $\tau\cdot\phi$, it suffices to replace g^2 by $\tau_1\cdot\tau_2g^2$; τ_1 and τ_2 are the isotopic spin operators referring to nucleons 1 and 2.

In solving for the phase shifts due to these one-boson-exchange potentials, one inserts the sum of potentials into the Schrödinger equation

$$-[\hbar^2/M]\nabla^2\Psi+\sum_\alpha V^{(\alpha)}(r)\Psi=E\Psi$$

and solves for the partial-wave scattering amplitudes. We take $M=938.5$ MeV, and $\hbar c=197.32$ MeV-F. All tabulated phase shifts are nuclear bar phase shifts as defined in Stapp, Ypsilantis, and Metropolis.[20]

III. THE NUCLEON-NUCLEON POTENTIAL

A. The Yale and Hamada-Johnston Phenomenological Potentials

There exist at present two up-to-date potential model representations of the 0- to 350-MeV nucleon-nucleon scattering data. These are the models due to Lassila, Hull, Ruppel, McDonald, and Breit,[21] henceforth referred to as "Yale," and the model due to Hamada and Johnston,[22] to be referred to as "HJ." Both the Yale and the HJ models reduce to the one-pion-exchange potential at large internucleon separation distances. We shall find these models extremely useful in the construction of our own many-one-meson-exchange potential.

First, however, we will want to eliminate a large quadratic spin-orbit potential which appears in each of these models, as none of the one-boson-exchange potentials we shall consider has a quadratic LS term of comparable strength. To eliminate the Yale and HJ quadratic LS potentials we shall simply replace the corresponding quadratic LS operators by a linear combination of central, tensor, and spin-orbit operators with coefficients chosen to yield the same matrix elements in either P or D states (whichever applies). This will, in effect, convert the quadratic LS potential into a sum of central, tensor, and spin-orbit potentials. These will be added to the original central, tensor, and spin-orbit potentials to yield a new potential which predicts the same P- and D-state phase shifts. We shall refer to this as the "modified" potential.

The modified version will of course predict different S, F, and G phase shifts than the original, but the F

[19] J. K. Perring and R. J. N. Phillips, Atomic Energy Research Establishment Report No. R 4077 Harwell, England, June, 1962 (unpublished); and R. Bryan (unpublished).

[20] H. P. Stapp, T. J. Ypsilantis, and N. Metropolis, Phys. Rev. 105, 302 (1957).

[21] K. E. Lassila, M. H. Hull, Jr., H. M. Ruppel, F. A. McDonald, and G. Breit, Phys. Rev. 126, 881 (1962).

[22] T. Hamada and I. D. Johnston, Nucl. Phys. 34, 382 (1962).

and G phases will not differ greatly because of the short range of the Yale and HJ quadratic forces. The S-state predictions will be different, of course, but this will not affect the present study, as we will be treating only P states and higher.

In the Yale model the quadratic spin-orbit potential appears only in even angular momentum states. The quadratic LS operator takes the form

$$\tfrac{1}{2}[(\boldsymbol{\sigma}_1 \cdot \mathbf{L})(\boldsymbol{\sigma}_2 \cdot \mathbf{L}) + (\boldsymbol{\sigma}_2 \cdot \mathbf{L})(\boldsymbol{\sigma}_1 \cdot \mathbf{L})] - (\mathbf{L} \cdot \mathbf{S})^2$$
$$= (\mathbf{L} \cdot \mathbf{S})^2 + \mathbf{L} \cdot \mathbf{S} - \mathbf{L}^2.$$

In the singlet spin states this operator is equivalent to $-\mathbf{L}^2$. Thus, the total potential acting in the $^1D_2$ state is $^1V_c - 6\,^1V_q$, to use the Yale group's notation. We define this sum to be the modified Yale potential in singlet even states.

In the case of the triplet even states, we replace the Yale quadratic LS operator by a linear combination of central, tensor, and spin-orbit operators which has the same matrix elements in triplet D states. This operator is $-2 \cdot \mathbf{1} - (7/4)S_{12} + \tfrac{1}{2}\mathbf{L} \cdot \mathbf{S}$. The modified potential in triplet even states thereby becomes

$$^3V^+ = {}^3V_c^+ \mathbf{1} + {}^3V_T^+ S_{12} + {}^3V_{LS}^+ \mathbf{L} \cdot \mathbf{S}$$
$$+ {}^3V_q^+ (-2 \cdot \mathbf{1} - (7/4)S_{12} + \tfrac{1}{2}\mathbf{L} \cdot \mathbf{S}).$$

One observes that the Yale potential is defined in terms of singlet and triplet spin projection operators, $S = \tfrac{1}{4}(1 - \boldsymbol{\sigma}_1 \cdot \boldsymbol{\sigma}_2)$ and $T = \tfrac{1}{4}(3 + \boldsymbol{\sigma}_1 \cdot \boldsymbol{\sigma}_2)$ so that the potential may be written

$$V = {}^1V_C S + ({}^3V_C \mathbf{1} + {}^3V_T S_{12} + {}^3V_{LS} \mathbf{L} \cdot \mathbf{S})T.$$

The one-boson-exchange potentials appear most simply using the operators $\mathbf{1}$ and $\boldsymbol{\sigma}_1 \cdot \boldsymbol{\sigma}_2$, however, so we will want to recast the Yale potential into the form

$$V = V_C \mathbf{1} + V_{\sigma\sigma} \boldsymbol{\sigma}_1 \cdot \boldsymbol{\sigma}_2 + V_T S_{12} + V_{LS} \mathbf{L} \cdot \mathbf{S} \qquad (3.1)$$

(with isotopic spin indices suppressed). This amounts to defining the central and spin-spin potentials V_C and $V_{\sigma\sigma}$ as

$$V_C = \tfrac{3}{4}\,{}^3V_C + \tfrac{1}{4}\,{}^1V_C$$

and

$$V_{\sigma\sigma} = \tfrac{1}{4}\,{}^3V_C - \tfrac{1}{4}\,{}^1V_C.$$

The one-boson-exchange potentials exhibit an isotopic spin dependence of the form

$$V^{(0)} + \boldsymbol{\tau}_1 \cdot \boldsymbol{\tau}_2 V^{(1)},$$

where only $T = 0$ mesons contribute to $V^{(0)}$ and only $T = 1$ mesons contribute to $V^{(1)}$. We will want to cast the Yale potential into this same form. This is equivalent to defining

$$V^{(0)} = \tfrac{3}{4}\,{}^{T=1}V + \tfrac{1}{4}\,{}^{T=0}V$$

and

$$V^{(1)} = \tfrac{1}{4}\,{}^{T=1}V - \tfrac{1}{4}\,{}^{T=0}V,$$

where $^{T=0}V$ and $^{T=1}V$ are the potentials which act, respectively, in nucleon-nucleon scattering states of

isotopic spin $T = 0$ and $T = 1$. Both $V^{(0)}$ and $V^{(1)}$ are understood to consist of linear combinations of central, spin-spin, tensor, and spin-orbit potentials, as in Eq. (3.1). The modified Yale potential thereby takes the form

$$V = V_C^{(0)} \mathbf{1} + V_{\sigma\sigma}^{(0)} \boldsymbol{\sigma}_1 \cdot \boldsymbol{\sigma}_2 + V_T^{(0)} S_{12} + V_{LS}^{(0)} \mathbf{L} \cdot \mathbf{S}$$
$$+ [V_C^{(1)} \mathbf{1} + V_{\sigma\sigma}^{(1)} \boldsymbol{\sigma}_1 \cdot \boldsymbol{\sigma}_2$$
$$+ V_T^{(1)} S_{12} + V_{LS}^{(1)} \mathbf{L} \cdot \mathbf{S}] \boldsymbol{\tau}_1 \cdot \boldsymbol{\tau}_2. \qquad (3.2)$$

This potential has been calculated by us and is graphed, in dashed lines, in Figs. 2 and 3.

Let us next consider the Hamada-Johnston potential. Since Hamada and Johnston have derived their model independently of the Yale group, using their own data selection, it will be interesting to see how closely their version agrees with Yale's. This will provide us with a measure of the reproducibility, or uniqueness, of these phenomenological representations of the nucleon-nucleon scattering data.

The HJ potential has a quadratic spin-orbit potential in both the even and the odd angular momentum states, in contrast to the Yale potential which has a quadratic LS term only in the even states. The version of the quadratic LS operator appearing in the Hamada-Johnston work is

$$L_{12} = (\boldsymbol{\sigma}_1 \cdot \boldsymbol{\sigma}_2)\mathbf{L}^2 - \tfrac{1}{2}[(\boldsymbol{\sigma}_1 \cdot \mathbf{L})(\boldsymbol{\sigma}_2 \cdot \mathbf{L}) + (\boldsymbol{\sigma}_2 \cdot \mathbf{L})(\boldsymbol{\sigma}_1 \cdot \mathbf{L})]$$
$$= -2(\mathbf{L} \cdot \mathbf{S})^2 - \mathbf{L} \cdot \mathbf{S} + \mathbf{L}^2 + (\boldsymbol{\sigma}_1 \cdot \boldsymbol{\sigma}_2)\mathbf{L}^2.$$

In singlet states L_{12} becomes simply $-2L^2$. Thus, the potentials acting in the singlet states of angular momentum L are

$$^1V^{\pm} = {}^1V_C^{\pm} - 2L(L+1){}^1V_{LL}^{\pm},$$

using Hamada and Johnston's notation. We will take as the modified version those singlet potentials

$$^1V^- = {}^1V_C^- - 4\,{}^1V_{LL}^-$$

and

$$^1V^+ = {}^1V_C^+ - 12\,{}^1V_{LL}^+,$$

thus choosing for the $^1P_1$, $^1F_3$, $\cdots$ states the interaction strength previously manifest in the P states, and for the $^1S_0$, $^1D_2$, $^1G_4$, $\cdots$ states the strength previously manifest in the $^1D_2$ state.

In the triplet spin states, the operator L_{12} becomes $-2(\mathbf{L} \cdot \mathbf{S})^2 - \mathbf{L} \cdot \mathbf{S} + 2\mathbf{L}^2$. A linear combination of operators which has the same matrix elements in the triplet P states is the quantity $\tfrac{4}{3}\mathbf{1} + \tfrac{5}{6}S_{12}$ (the LS operator happens to have zero coefficient). We take as the modified version of the HJ potential for triplet odd states

$$^3V^- = {}^3V_C^- \mathbf{1} + {}^3V_T^- S_{12} + {}^3V_{LS}^- \mathbf{L} \cdot \mathbf{S} + {}^3V_{LL}^- (\tfrac{4}{3} \cdot \mathbf{1} + \tfrac{5}{6}S_{12}).$$

For the triplet D states, the linear combination of operators which yields the same matrix elements as L_{12} is the operator $4 \cdot \mathbf{1} + \tfrac{7}{2}S_{12}$. Therefore we shall take as the effective Hamada-Johnston potential for triplet
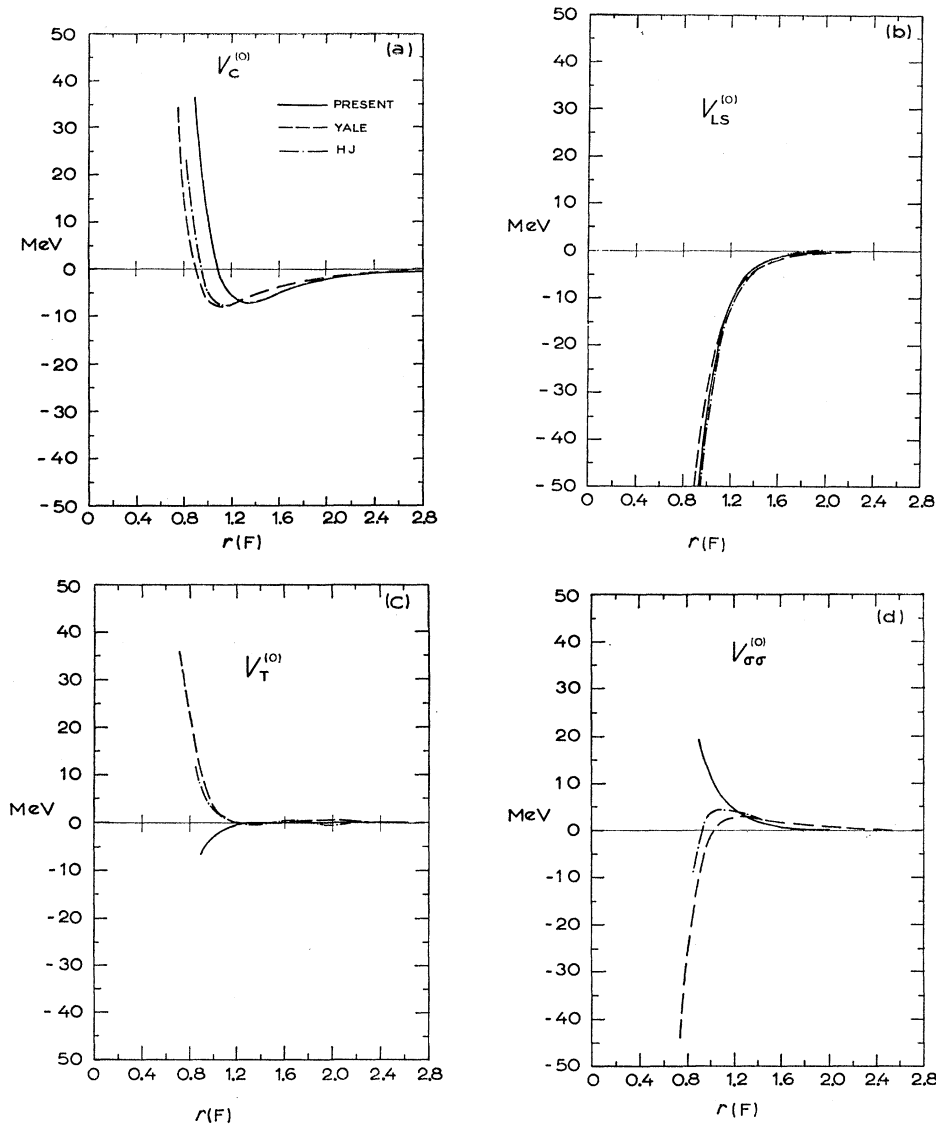
FIG. 2. The predicted isoscalar potential $V^{(0)}$ (present) as compared with the modified Yale and Hamada-Johnston (HJ) potentials (see text). The HJ curve is suppressed where it falls exactly on the Yale curve.

even states

$$^3V^+ = {}^3V_C + 1 + {}^3V_T + S_{12} + {}^3V_{LS} + \mathbf{L} \cdot \mathbf{S} + {}^3V_{LL} + (4 \cdot 1 + \tfrac{7}{2}S_{12}).$$

The modified HJ potential is cast in the form of Eq. (3.2). This potential has been calculated by us and is presented in Figs. 2 and 3 in the form of alternately long- and short-dashed lines.

Note how closely the Yale and HJ potentials agree. It appears that Lassila *et al.* and Hamada and Johnston have found a single-potential model solution to the nucleon-nucleon scattering data.

B. The N-N Isoscalar Potential and the $T=0$ Mesons

Let us first consider the $T=0$ mesons and the phenomenological isoscalar potential $V^{(0)}$. It is desired to adjust the meson parameters such that the sum of

corresponding one-boson-exchange potentials reproduces the empirical Yale and Hamada-Johnston potentials. Actually, agreement will only be required for internucleon distances greater than one F. S waves will not be treated in this analysis, and the next most sensitive waves to the inner region, P waves, impact no closer than one F at the highest energy treated in this analysis (320 MeV). Further discussion on the insensitivity of P waves and higher to the inner interaction may be found in Sec. IV.

The mesons whose OBEP are to match the isoscalar phenomenological potentials are the η, the σ_0, and the ω. From examination of the formulas for these OBEP, given in Sec. II one sees that the ω OBEP includes all four types of terms to be found in this nonrelativistic analysis—1, $\mathbf{L} \cdot \mathbf{S}$, S_{12}, $\sigma_1 \cdot \sigma_2$—but that the σ_0 OBEP and the η OBEP include just two terms each, 1 and $\mathbf{L} \cdot \mathbf{S}$ for
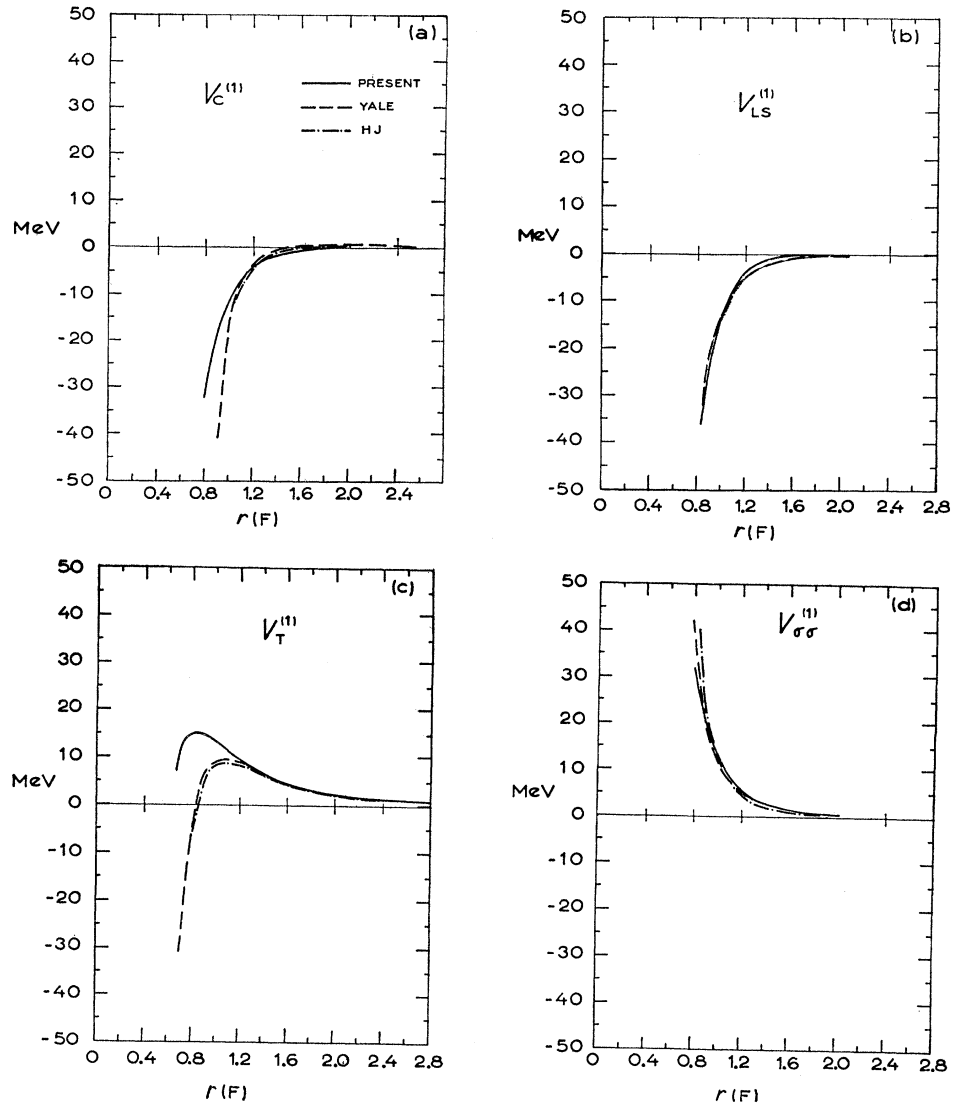
FIG. 3. The predicted isovector potential $V^{(1)}$ (present) as compared with the modified Yale and Hamada-Johnston potentials. The HJ curve is suppressed when it falls exactly on the Yale curve, as is the Yale curve when it falls exactly on the curve "present."

the σ_0, and S_{12} and $\sigma_1 \cdot \sigma_2$ for the η. Thus, the central and spin-orbit potentials are to be given by just the OBEP of the ω and the σ_0 and the tensor and spin-spin potentials by just the OBEP of the ω and the η. These qualitative facts appear in Table I. The quantum numbers and masses of the bosons are taken from the current literature such as summarized in the reports of Roos[23] and Barkas and Rosenfeld.[24]

Let us first study the "experimental" potentials $V_T^{(0)}$ and $V_{\sigma\sigma}^{(0)}$. These phenomenological forms are to be reproduced by the S_{12} and $\sigma_1 \cdot \sigma_2$ terms of the η and ω OBEP. The leading contributing terms are

$$V_T^{(0)} = -g_\omega^2 \tfrac{1}{4}(m_\omega^2/M^2)\chi(m_\omega r)m_\omega$$
$$+ g_\eta^2 \tfrac{1}{4}(m_\eta^2/M^2)\chi(m_\eta r)m_\eta$$

[23] M. Roos, Rev. Mod. Phys. 35, 314 (1963).
[24] W. H. Barkas and A. H. Rosenfeld, Lawrence Radiation Laboratory Report, UCRL Report 8030 Rev., April, 1963 edition (unpublished).

and

$$V_{\sigma\sigma}^{(0)} = g_\omega^2 \tfrac{1}{6}(m_\omega^2/M^2)\Phi(m_\omega r)m_\omega$$
$$+ g_\eta^2 \tfrac{1}{12}(m_\eta^2/M^2)\Phi(m_\eta r)m_\eta,$$

where we neglect derivative coupling for the ω. Examination of the Yale and HJ potentials, graphed

TABLE I. Bosons listed under the terms to which they contribute in the one-boson-exchange potential approximation. Boson quantum numbers[a] and mass listed to the right of the particle.

$V_C^{(0)}$	$V_{LS}^{(0)}$	$V_T^{(0)}$	$V_{\sigma\sigma}^{(0)}$	$V_C^{(1)}$	$V_{LS}^{(1)}$	$V_T^{(1)}$	$V_{\sigma\sigma}^{(1)}$	T	J^{PG}	mass
...	...	η	η	...	...	...	...	0	0^{-+}	$3.9m_\pi$
σ_0	σ_0	...	...	...	...	...	...	0	0^{++}	?
ω	ω	ω	ω	...	...	...	...	0	1^{--}	$5.6m_\pi$
...	...	...	...	...	...	π	π	1	0^{--}	$1.0m_\pi$
...	...	...	...	σ_1	σ_1	...	...	1	0^{+-}	?
...	...	...	...	ρ	ρ	ρ	ρ	1	1^{-+}	$5.4m_\pi$
ϕ	ϕ	ϕ	ϕ	...	...	...	...	0	1^{--}	$7.3m_\pi$

[a] G parity is such that every meson listed may be emitted at a nucleon vertex.
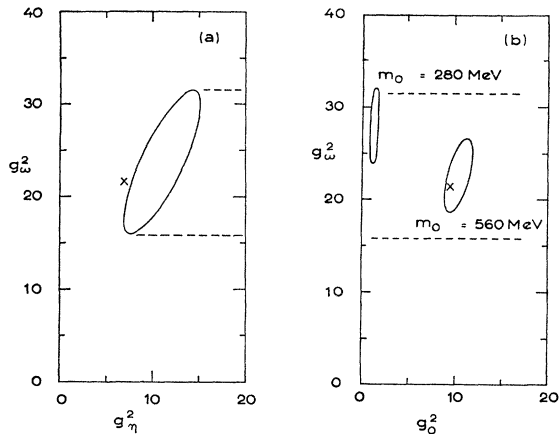
FIG. 4. Ellipses bounding the region of correlated isoscalar meson-nucleon coupling constants as predicted from fitting phenomenological potentials. The "$\times$"'s denote the values obtained after fitting experimental phase shifts.

in Figs. 2(c) and 2(d) as dashed and dash-dotted lines, respectively, shows that for $r > 1$ F the tensor potential vanishes and the spin-spin potential is positive. The one-boson-exchange potentials above can satisfy these requirements: The two S_{12} terms above have opposite signs plus sufficiently equal range ($m_\omega = 5.6 m_\pi$, $m_\eta = 3.9 m_\pi$), and the two $\sigma_1 \cdot \sigma_2$ terms are both positive. Some work with a desk calculator reveals that the values of g_η^2 and g_ω^2 which allow the best match between theory and experiment are approximately 11 and 23, respectively. The latitude in this estimate is indicated by means of Fig. 4(a), where g_η^2 and g_ω^2 are taken to be "x" and "y" coordinates and the most probable correlated values for g_η^2 and g_ω^2 span the area within the ellipse.

Let us now consider the remaining isoscalar potentials $V_C^{(0)}$ and $V_{LS}^{(0)}$. These are to be due to the OBEP of the ω and the σ_0. The Yale and Hamada-Johnston versions, graphed in Figs. 2(a) and 2(b), show a strong short-ranged attraction for $V_{LS}^{(0)}$ and a strong short-ranged repulsion for $V_C^{(0)}$. These effects are characteristic of the exchange of the $J = 1^- \omega$; furthermore the mass of the ω, 782 MeV, is correct for the empirically determined range of $V_{LS}^{(0)}$. However, there is some difficulty in fitting the isoscalar central potential. Empirically, the strong repulsion at short distances gives way to a mild attraction at intermediate distances (the source of the binding of nuclear matter). Apparently some other process has come into play. In keeping with the spirit of the "pole" model, we assume this to be due to the exchange of a new meson. In particular, we assume this meson has quantum numbers $T = 0$, $J = 0^+$, as the OBEP of such a meson has an attractive central term.[25] (The next lowest quantum numbers for

[25] Gupta has also postulated a $T = 0$, $J = 0^+$ meson [S. N. Gupta, Phys. Rev. Letters **2**, 124 (1959)], but on the basis that such a meson provides an attractive LS force. In our model, the σ_0 provides only about $\frac{1}{4}$ of the isoscalar LS force.

a meson giving rise to a central attraction are 2^+, for the OBEP of 0^- and 1^+ mesons do not *have* a central term.[17]) Let us designate the postulated meson σ_0. Some experimental evidence in its favor is discussed in Sec. V.

The coupling constants of the ω and σ_0 and also the mass of the σ_0, are to be adjusted such that the OBEP reproduce the phenomenological central and spin-orbit potentials. The appropriate formulas are, to lowest order,

$$V_C^{(0)} = g_\omega^2 \Phi(m_\omega r) m_\omega - g_0^2 \Phi(m_0 r) m_0$$

and

$$V_{LS}^{(0)} = g_\omega^2 \tfrac{3}{2} (m_\omega^2 / M^2) J(m_\omega r) m_\omega$$
$$+ g_0^2 \tfrac{1}{2} (m_0^2 / M^2) J(m_0 r) m_0 ,$$

where the mass and coupling constant of the σ_0 are m_0 and g_0, respectively. m_0 must be lower than m_ω in order to give an attraction in $V_C^{(0)}$ of longer range than the repulsion, but it must also be greater than $2m_\pi$ to agree with the range as given by Yale or Hamada-Johnston. Some desk calculator work shows that a mass of $m_0 = 4m_\pi$ seems about right, for which g_ω^2 and g_0^2 are about 23 and 10, respectively, but if we take $m_0 = 2m_\pi$, then g_ω^2 and g_0^2 are about 28 and 1, respectively. Fig. 4(b) gives further information. The most likely correlated values for g_ω^2 and g_0^2 are to be found within the ellipses.

It is reassuring to note that the values of g_ω^2 just determined are reasonably independent of the mass of the σ_0. The reason for this is that the ω OBEP makes the largest contribution to the LS potential so variations in the σ_0 contribution do not vary the ω contribution, i.e., g_ω^2, very much percentagewise.

In summing up the results of the three OBEP fit to the isoscalar phenomenological potentials, the most significant points seem to be (1) that the OBEP of the η, the ω and the σ_0 can indeed fit the Yale and Hamada-Johnston curves, and (2) that the ω-nucleon coupling constant determined through the $V_C^{(0)}$-$V_{LS}^{(0)}$ fit is consistent with the value determined through the $V_{\sigma\sigma}^{(0)}$-$V_T^{(0)}$ fit. That is, the ellipses in Fig. 4(b) fall almost entirely within the dashed lines depicting the maximum extent of the ellipse in Fig. 4(a). Apparently derivative coupling is not needed for the ω. One set of approximate values for the η, ω, and σ_0 which produce a fit to the empirical potentials in Born approximation are $g_\omega^2 = 23$, $g_\eta^2 = 11$, $g_0^2 = 10$, and $m_0 = 4m_\pi$.

C. The N-N Isovector Potentials and the $T = 1$ Mesons

The N-N isovector potential is assumed to be given by the sum of the one-boson-exchange potentials of three $T = 1$ mesons: the π, the ρ, and the $J = 0^+ \sigma_1$. The gross features of these OBEP are listed in Table I. Note that the ρ OBEP contributes to $V_C^{(1)}$, $V_{LS}^{(1)}$, $V_T^{(1)}$, and $V_{\sigma\sigma}^{(1)}$, but that the π OBEP contributes only to $V_T^{(1)}$ and $V_{\sigma\sigma}^{(1)}$, and that the σ_0 OBEP only to $V_C^{(1)}$ and

$V_{LS}^{(1)}$. Thus, the ρ and the π are the source of $V_T^{(1)}$ and $V_{\sigma\sigma}^{(1)}$, while the ρ and the σ_1 are the source of $V_C^{(1)}$ and $V_{LS}^{(1)}$.

The potentials $V_T^{(1)}$ and $V_{\sigma\sigma}^{(1)}$ will be considered first. The appropriate meson theory contributions are

$$V_T^{(1)} = -g_\rho^2 R_{12}(f_\rho/g_\rho)\tfrac{1}{4}(m_\rho^2/M^2)\chi(m_\rho r)m_\rho$$
$$+g_\pi^2\tfrac{1}{4}(m_\pi^2/M^2)\chi(m_\pi r)m_\pi$$

and

$$V_{\sigma\sigma}^{(1)} = g_\rho^2 R_{12}(f_\rho/g_\rho)\tfrac{1}{6}(m_\rho^2/M^2)\Phi(m_\rho r)m_\rho$$
$$+g_\pi^2\tfrac{1}{12}(m_\pi^2/M^2)\Phi(m_\pi r)m_\pi.$$

Observe that the ρ meson has been assumed to couple to the nucleon both "electrically" and "magnetically," as evidenced by the term R_{12} in the above equations. (See Sec. II for definitions.) This more general coupling turns out to be necessary in order for the ρ OBEP to fit the empirical $V_C^{(1)}$ and $V_{LS}^{(1)}$ potentials as well as the empirical $V_T^{(1)}$ and $V_{\sigma\sigma}^{(1)}$ potentials. Insofar as the present treatment of $V_T^{(1)}$ and $V_{\sigma\sigma}^{(1)}$ is concerned, however, it will only be necessary to search for the best value of the product $g_\rho^2 R_{12}$—the determination of individual terms g_ρ^2 and R_{12} need be carried out only after we analyze $V_C^{(1)}$ and $V_{LS}^{(1)}$.

The Yale and Hamada–Johnston work indicates that $V_T^{(1)}$ is attractive at short distances, but has a positive, long-range tail, and that $V_{\sigma\sigma}^{(1)}$ is always positive, but decreases rapidly with distance. These features may be observed in Figs. 3(c) and 3(d), in which the Yale and the Hamada-Johnston potentials are graphed as dashed and dash-dotted lines, respectively. The characteristics of these empirical potentials can be reproduced qualitatively by the π and the ρ one-boson-exchange potentials; i.e., for the tensor potential, the π OBEP provides a long-range repulsion (this comes as no surprise—the Yale and HJ versions incorporate the π OBEP) while the ρ OBEP provides a short-range attraction, and in the case of the spin-spin potential, both mesonic contributions are positive. There is some slight trouble in achieving a quantitative fit, however. When $g_\rho^2 R_{12}$ is adjusted to provide sufficient short-range negative cancellation of the tensor force of the π meson OBEP, the concomitant spin-spin contribution is too positive. Still, a not unreasonable compromise is possible for $g_\rho^2 R_{12} \approx 30$ and $g_\pi^2 \approx 11$. Other possible correlated values for g_π^2 and $g_\rho^2 R_{12}$ are indicated in Fig. 5(a) as falling within the boundary of the plotted ellipse. Note that the range of values for g_π^2 is somewhat below the customarily quoted figure of 14 to 15.

There remain the central and spin-spin potentials to be determined. The Yale and Hamada-Johnston versions of these potentials are graphed in Figs. 3(a) and 3(b). Observe that both $V_C^{(1)}$ and $V_{LS}^{(1)}$ are attractive and quite short-ranged. The short-range attraction in the spin-orbit potential may be ascribed in a natural way to the ρ OBEP. Not only is the ρ contribution of the right sign, but the range is also correct. The short-
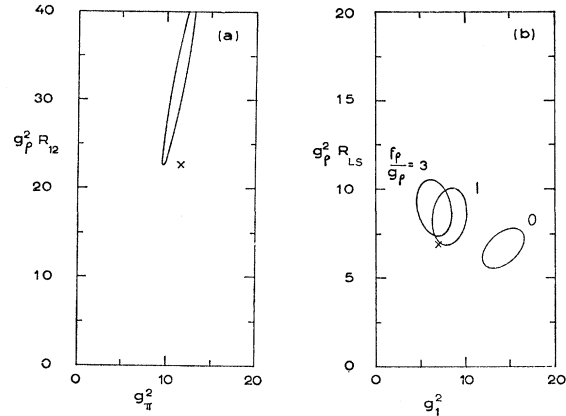

FIG. 5. Ellipses bounding the region of correlated isovector meson-nucleon coupling constants as predicted from fitting phenomenological potentials. The "$\times$"'s denote the values obtained after fitting experimental phase shifts.

range attraction in $V_C^{(1)}$, however, is something of a mystery. The ρ OBEP contribution must necessarily be repulsive, and no other known meson contributes here in Born approximation. We are lead therefore to introduce another meson, or one-boson-exchange potential, to provide the required attraction in the central potential. The choice of quantum numbers is again 0^+, 2^+, and other states with $J \geq 2$ as discussed before in connection with the conjecture of the σ_0. As before, we select the quantum number 0^+, as $J=0$ is the lowest value consistent with our requirements. The mass of the meson should be in the range of $5.5m_\pi$ in order to provide the correct short-range attraction. Let us designate this meson the σ_1, in analogy to the σ_0 previously introduced. Further discussion on the σ_1 may be found in Sec. V.

The ρ and the σ_1 contribute in Born approximation to $V_C^{(1)}$ and $V_{LS}^{(1)}$ as follows:

$$V_C^{(1)} \approx g_\rho^2 R_C (f_\rho/g_\rho)\Phi(m_\rho r)m_\rho - g_1^2\Phi(m_1 r)m_1$$

and

$$V_{LS}^{(1)} \approx g_\rho^2 R_{LS}(f_\rho/g_\rho)\tfrac{3}{2}(m_\rho^2/M^2)J(m_\rho r)m_\rho$$
$$+g_1^2\tfrac{1}{2}(m_1^2/M^2)J(m_1 r)m_1,$$

where g_1 and m_1 are the σ_1 coupling constant and mass, respectively.

The factors R_C and R_{LS} arise as a consequence of taking both direct and derivative coupling for the ρ meson. These functions are defined in Sec. II and graphed in Fig. 1 over the range $-4 < f_\rho/g_\rho < 4$. In fitting the OBEP to empirical potentials $V_C^{(1)}$ and $V_{LS}^{(1)}$ it will be necessary to search for both $g_\rho^2 R_C$ and $g_\rho^2 R_{LS}$, or alternately, for both g_ρ^2 and f_ρ/g_ρ. For the present, however, we shall assume that $f_\rho/g_\rho = 0$, corresponding to the case of direct coupling only. Some desk calculator work then reveals that the Yale and Hamada–Johnston potentials can be reasonably fit taking $g_\rho^2 \approx 6$ and $g_1^2 \approx 14$ with $m_1 = 770$ MeV. Recalling

that $R_C = R_{LS} = R_{12} = 1$ for $f_\rho/g_\rho = 0$, we see that this fit predicts $g_\rho^2 R_{12} = 6$. But this result is clearly at variance with the determination of $g_\rho^2 R_{12}$ from the analysis of $V_T^{(1)}$ and $V_{\sigma\sigma}^{(1)}$ where it was found to be approximately 30.

Apparently direct coupling alone for the ρ meson is incompatible with a simultaneous fit to all four isovector potentials. What is required, rather, is an enhancement of the ρ tensor contribution with respect to the spin-orbit contribution. This is possible and occurs for $f_\rho/g_\rho = 1$, 2, 3 or more, as may be seen in Fig. 1. For each ratio f_ρ/g_ρ, one redetermines g_ρ^2 and g_1^2 by fitting the Yale and HJ potentials $V_C^{(1)}$ and $V_{LS}^{(1)}$. One then computes $g_\rho^2 R_{12}$ and compares it with 30—the prediction from the tensor and spin-spin analysis.

It turns out that indeed reasonable values for $g_\rho^2 R_{12}$ are to be found for f_ρ/g_ρ in the range $1 < f_\rho/g_\rho < 3$. Negative values for f_ρ/g_ρ do not lead to useful results: With $f_\rho/g_\rho < -2.9$, $g_\rho^2 R_{12}$ is much too large. For $-2.9 < f_\rho/g_\rho < -0.3$, R_{LS} is negative and g_ρ^2 assumes negative, thereby unphysical, values.

A set of parameters for the ρ which leads to a reasonably good fit to all four phenomenological isovector potentials is $f_\rho/g_\rho = 2$ and $g_\rho^2 = 0.7$. The corresponding σ_1 parameters are $g_1^2 = 7$ and $m_1 = 770$ MeV. The mass of the σ_1 is taken to be 770 MeV in order to yield the range of the empirical $V_C^{(1)}$. Actually m_1 could vary as much as 150 MeV either up or down.

In Fig. 5(b) there are plotted ellipses circumscribing the estimated correlated values for $g_\rho^2 R_{LS}$ and g_1^2 for $f_\rho/g_\rho = 0$, 1, and 3, and one may observe that $g_\rho^2 R_{LS}$ is reasonably independent of g_1^2. A similar graph, but for $m_1 = 560$ MeV (not shown), indicates that $g_\rho^2 R_{LS}$ assumes nearly the same values for each ratio f_ρ/g_ρ as it does in the case of $m_1 = 770$ MeV. Thus, the ρ analysis is insensitive to the mass of the σ_1. It therefore appears that the parameters thus deduced for the ρ are independent of the σ_1 hypothesis much as the ω parameters are independent of the σ_0 hypothesis.

In summing up, the analysis of Sec. III reveals the following facts: It is possible to fit the modified Yale and Hamada-Johnston isovector potentials with the π, ρ, and σ_1 OBEP, just as it is possible to fit the isoscalar potentials with the η, ω, and σ_0 OBEP. In each case, it proves necessary to introduce a scalar meson, the $T = 1$ σ_1 for the isovector potentials, and the $T = 0$ σ_0 for the isoscalar potentials. One difference in the two analyses is that it proves necessary to introduce derivative coupling for the ρ but not so for the ω. Apparently, the nucleon-nucleon data are consistent with zero "magnetic" coupling for the ω. One set of parameters which allows a fit to the nucleon-nucleon empirical potentials is $g_\eta^2 = 11$, $g_\omega^2 = 23$, $f_\omega/g_\omega = 0$, $g_0^2 = 10$, $m_0 = 4m_\pi$, $g_\pi^2 = 11$, $g_\rho^2 = 0.73$, $f_\rho/g_\rho = 2$, $g_1^2 = 7$, and $m_1 = 5.5m_\pi$.

IV. THE NUCLEON-NUCLEON PHASE SHIFTS

The second phase of the research is the adjustment of the poles to fit the experimentally determined phase shifts over the 0- to 320-MeV laboratory scattering energy range. The determination in the previous section of the necessary number of mesons and concomitant parameters provides a useful starting point. Indeed, if the preceding fit to the potential models is valid, additional adjustment of the parameters should be minor.

It is fortunate that there is an abundance of nucleon-nucleon data over the nonrelativistic scattering energy range, and that these data have been reduced to a unique set of phase shifts through the combined efforts of several different groups. A principal factor in achieving this unique solution has been the introduction by Moravcsik[16] of his modified method of analysis in which the higher partial waves are given by the pion pole contribution. This single solution for the lower partials is commonly referred to as "type 1," at least for the $T = 1$ states. In the $T = 0$ states there has appeared in the literature just one solution consistent with the $T = 1$ type 1 solution. (Actually, there exists another $T = 1$ solution, called "type 2." This solution crops up at some energies, but type 1 is the only solution which can be realistically extended over the entire 0- to 320-MeV range.)

For our pole fit, we select the following type 1 modified phase-shift solutions to represent the experimental data:

(1) A $T = 1$ energy-dependent solution spanning the 10- to 345-MeV range due to Breit, Hull, Lassila, Pyatt, and Ruppel.[26] This solution is called YLAM by the authors, and we shall refer to it likewise. The authors assume $g_\pi^2 = 14$. This solution is graphed as a dashed line in Figs. 6, 7, and 8, for the P, D, and F states, respectively. The other phase-shift solutions to be listed below will also be graphed in Figs. 6 through 8 for P through F states.

(2) A $T = 0$ energy-dependent solution to go with the $T = 1$ solution YLAM. This solution, due to Hull, Lassila, Ruppel, McDonald, and Breit,[27] spans the 14- to 350-MeV range. The authors designate this solution YLAN3M and we shall likewise. It is graphed as a dashed line.

(3) A $T = 1$, 0- to 400-MeV energy-dependent solution due to Stapp, Noyes, and Moravcsik.[28] The authors provide a family of similar solutions and we select the one designated MIDPOP 1103 as this one seems to have the most reasonable energy dependence. This solution is graphed as a dash-dot curve.

[26] G. Breit, M. H. Hull, Jr., K. E. Lassila, and K. D. Pyatt, Jr., Phys. Rev. **120**, 2227 (1960); **128**, 826 (1962).

[27] M. H. Hull, Jr., K. E. Lassila, H. M. Ruppel, F. A. McDonald, and G. Breit, Phys. Rev. **122**, 1606 (1961); **128**, 830 (1962).

[28] H. P. Stapp, H. P. Noyes, and M. J. Moravcsik (to be published). We wish to thank Dr. Moravcsik for making available to us the results of this analysis prior to publication.
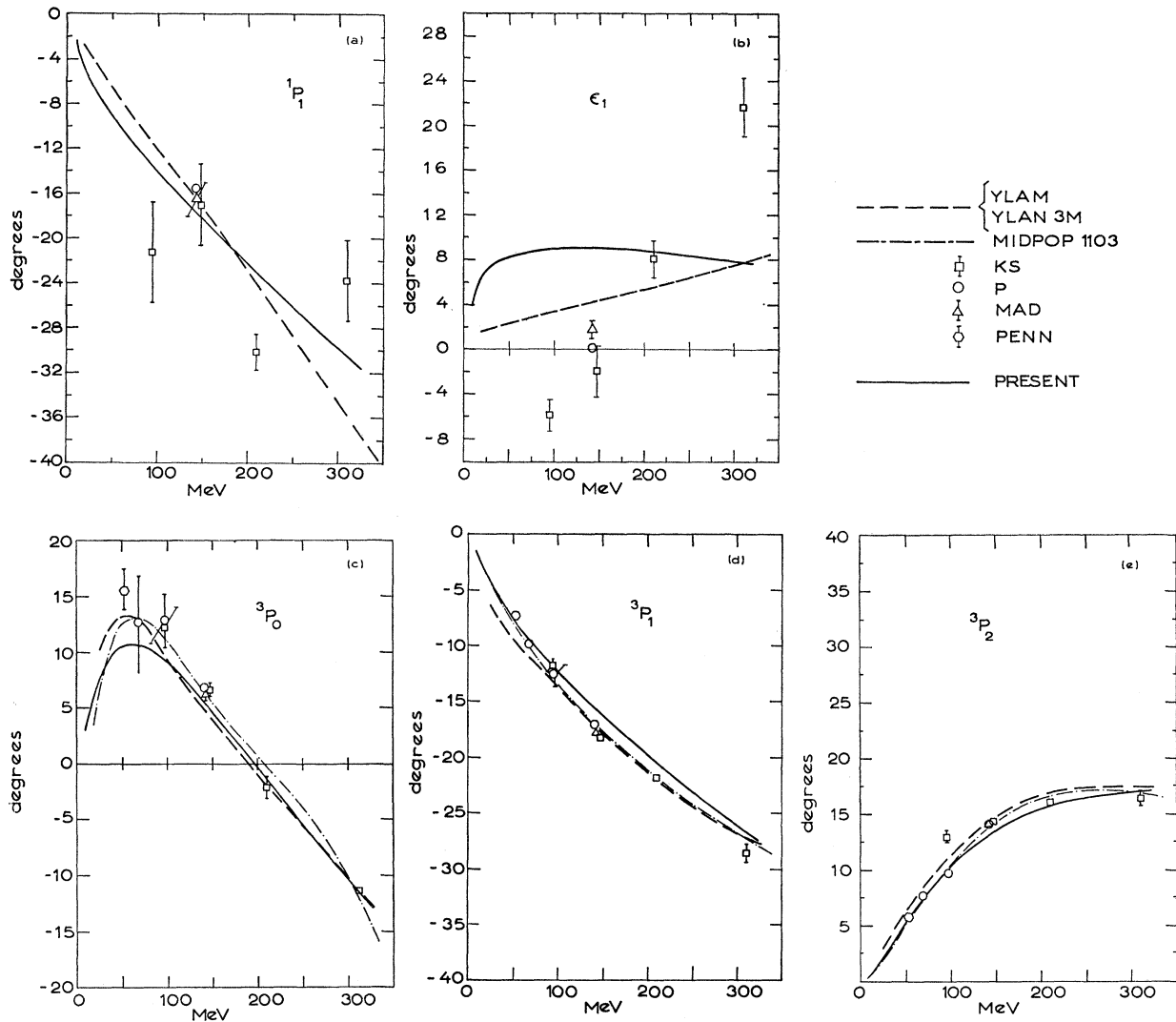
FIG. 6. Predicted nucleon-nucleon P phase parameters (present) as compared with several phase shift analyses over the 0- to 320-MeV energy range (see text); nuclear bar parametrization is employed.

(4) A series of single-energy solutions due to Kazarinov and Silin.[29,30] These are simultaneous $T=1$ and $T=0$ solutions. We select solutions at 95, 147, 210, and 310 MeV, designated by the authors as "Set 1a," "Set 1 (f^2 fixed)," "Set 1," and "Set 1," respectively, in Ref. 30. The pion-nucleon coupling constant is searched upon and found to be 12.8 ± 1.5, 14.4 ± 0.8, and 16.2 ± 1.3 at 95, 210, and 310 MeV, respectively. At 147 MeV, g_π^2 is fixed at 14.4. (However, the authors list another type 1 solution at this energy wherein g_π^2 is searched upon and found to be 11.6 ± 1.2. We list this information because it will be useful later in estimating the range of g_π^2 predicted by the higher nucleon-nucleon

partial waves.) These solutions are designated "KS" and are plotted as square symbols.

(5) A series of single energy solutions due to Perring.[31] He provides $T=1$ solutions at several energies, and we select the solutions at 68.3 and 98 MeV identified in Ref. 31 as "Solution 1" and "Solution 1a (seven parameter)," respectively. g_π^2 is taken to be 14. Perring also provides a combined $T=1$ and $T=0$ solution at 142 MeV.[32] We select the solution with twelve $T=1$ parameters. g_π^2 is again assumed to be 14. The Perring solutions are plotted as circles and are designated "P."

(6) A single-energy combined $T=1$ and $T=0$ solution at 142 MeV due to MacGregor, Arndt, and Dubow.[33] We select the solution designated DECK D in

[29] Y. M. Kazarinov and I. N. Silin, Zh. Eksperim. i Teor. Fiz. 43, 692 (1962) [English transl.: Soviet Phys.—JETP 16, 491 (1963)].
[30] Y. M. Kazarinov and I. N. Silin, Zh. Eksperim. i Teor. Fiz. 43, 1385 (1962) [English transl.: Soviet Phys.—JETP 16, 983 (1963)].
[31] J. K. Perring, Nucl. Phys. 30, 424 (1962).
[32] J. K. Perring, Nucl. Phys. 42, 306 (1963).
[33] M. H. MacGregor, R. A. Arndt, and A. A. Dubow (to be published).
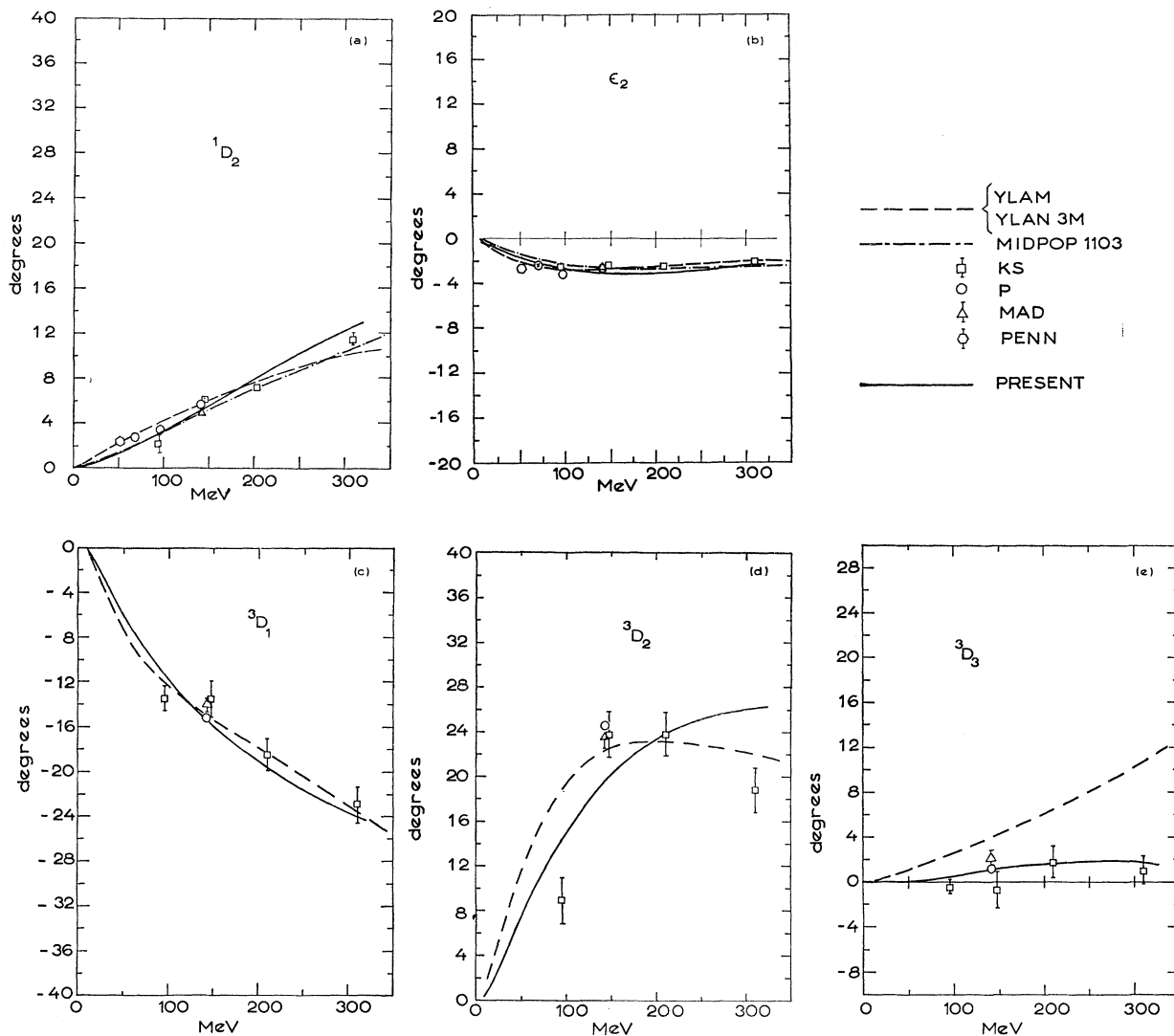
FIG. 7. Predicted nucleon-nucleon D-phase parameters (present) as compared with several phase shift analyses over the 0- to 320-MeV energy range.

Table X of Ref. 33. $g_\pi{}^2$ is a search parameter and takes the value 13.0. This solution is designated MAD and is plotted as triangles.

(7) A single-energy $T=1$ solution at 51.8 MeV due to Signell, Yoder, and Miskovsky.[34] We select their solution OPE(6) and plot it as hexagons. Also of note is a $T=1$ solution at 142 MeV due to Signell and Marker,[35] designated OPE(11) by them. We would plot this solution but there is not sufficient space. However, it can be stated that this solution is very close to the MacGregor, Arndt, and Dubow solution. We shall refer to both the aforementioned solutions as PENN. $g_\pi{}^2$ is taken to be 14.4 at both energies. (Note, however,

that when $g_\pi{}^2$ is released in the 142-MeV search, it assumes the value 11.8 ± 2.5, according to Fig. 13 of Ref. 35.)

The picture that emerges from an over-all view of the combined analyses as graphed in Figs. 6, 7, and 8 is that of a well-defined $T=1$ solution—to within a degree or two in nearly every instance—and a less well defined but still unique $T=0$ solution—with the most poorly defined states being the $^1P_1$, ϵ_1, $^3D_3$, and $^1F_3$. This data is nevertheless sufficient to provide a stringent test of the pole model, much more stringent, incidently, than provided by the phenomenological potential data in the previous section.

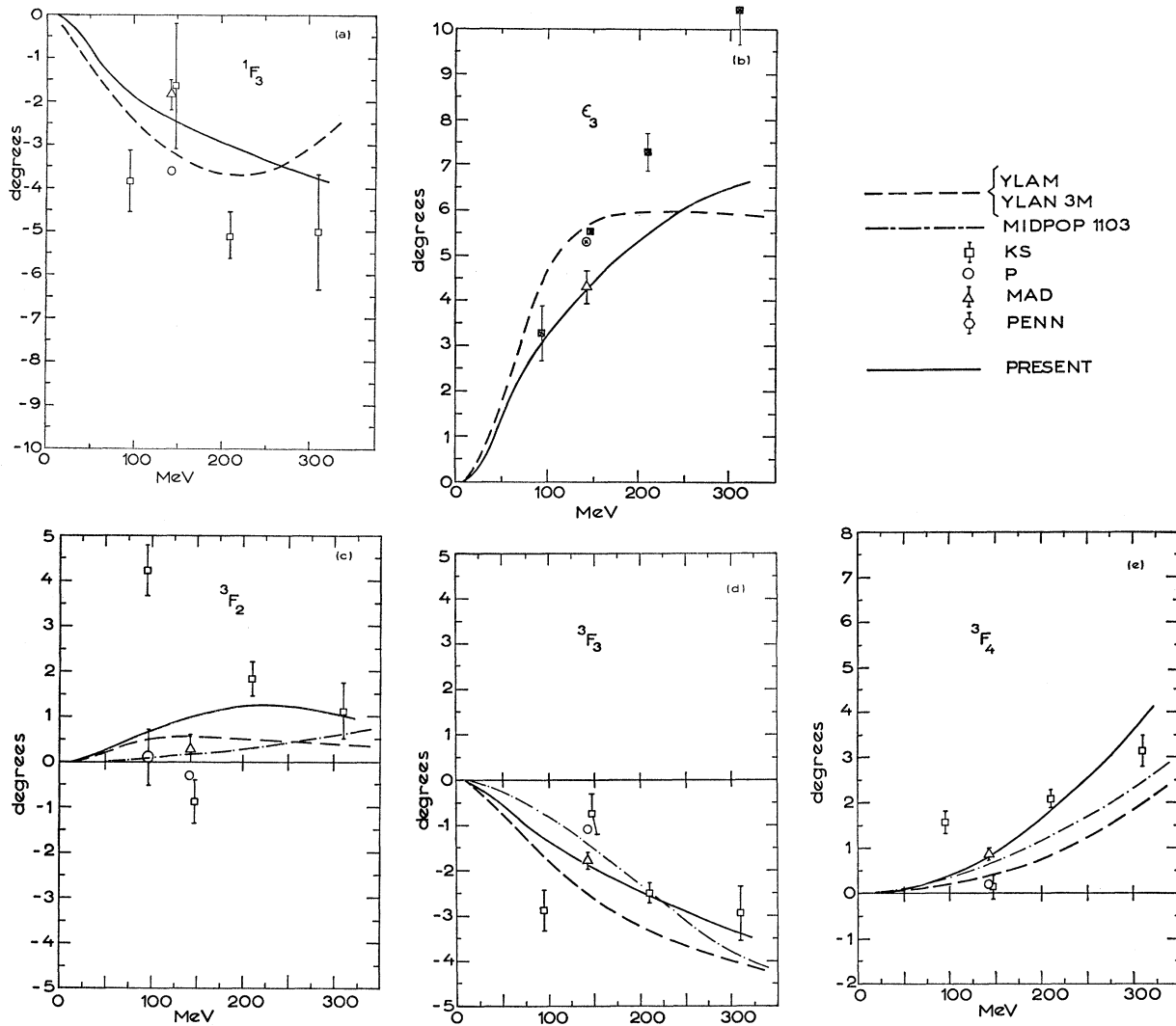Let us now consider some aspects of the use of the Schrödinger equation to generate unitarity. The partial-

[34] P. Signell, N. R. Yoder, and N. M. Miskovsky (to be published).
[35] P. Signell and D. L. Marker, Phys. Rev. 134, B365 (1964).

FIG. 8. Predicted nucleon-nucleon F-phase parameters (present) as compared with several phase shift analyses over the 0- to 320-MeV energy range.

wave equations are solved by a Runge-Kutta numerical integration procedure on a Minneapolis Honeywell 800 digital computer. Nuclear bar phase shifts are found by matching the computed wave functions to Coulomb functions for $T=1$ states ($\hbar c/e^2 = 137.04$) and to spherical Bessel functions for $T=0$ states at a maximum radius, so chosen that all significant contributions of the OBEP are obtained. Mesh widths of 0.02 from 0 to 1.0 F, and 0.05 from 1.0 to the maximum radius are used for all runs presented. It is found that all phase shifts thereby obtained are accurate to better than 0.5% with the exception of ϵ_1, which may be accurate only to 1% in some instances.

Actually, the Schrödinger equation cannot always be solved using the one-boson-exchange potentials. For the parameters, estimated in Sec. III, the Schrödinger equation is insoluble in the $^3P_2$ and $^3F_4$ states. This is

due to the $1/r^3$ singularity in the OBEP tensor and spin-orbit parts, and the fact that the matrix elements in the $^3P_2$ and $^3F_4$ states lead to an attractive potential at the origin.

Physically meaningful phase shifts can still be obtained for the states, however, through the use of cutoff. Fig. 9 illustrates the effect of one type of cutoff in which the complete potential is set to zero within a distance z_0, left unchanged beyond z_0. The phase shifts plotted in Figs. 9(a), (b), and (c) are the P, D, and F states, respectively. The calculation is carried out at 320 MeV, using for definiteness the pole parameters to be ultimately determined in this paper (presented in Table II). It may be seen that P phase shifts are insensitive to variations in z_0 so long as it is less than 0.5 F (with the exception of the $^3P_2$ state), similarly that D phase shifts are insensitive so long as z_0 is less than 0.7 F, and
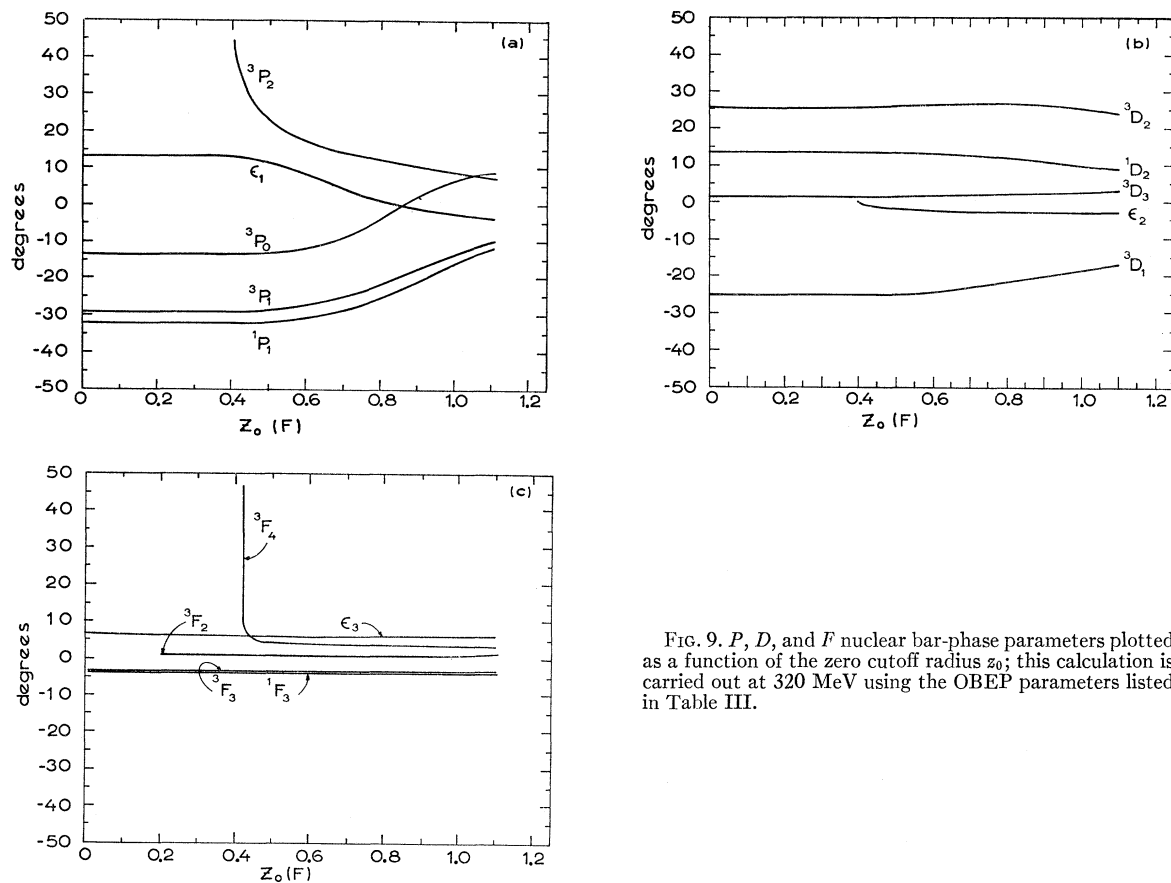
Fig. 9. P, D, and F nuclear bar-phase parameters plotted as a function of the zero cutoff radius z_0; this calculation is carried out at 320 MeV using the OBEP parameters listed in Table III.

similarly that F states are insensitive so long as z_0 is less than 1.1 F or more (with the exception of the $^3F_4$ state).

The $^3F_4$ state is also stable so long as z_0 exceeds 0.5 F. Within that distance this state is bound and the phase shift jumps through 180°, a phenomenon familiar from the work of Levinson.[36] By taking $z_0 > 0.5$ F, however, one preserves the Born character of the phase shift.

The $^3P_2$ phase shift exhibits similar behavior although there is not such a flat plateau in the value of the phase shift beyond 0.5 F. Such a flat plateau does exist even for the $^3P_2$ state, however, when the calculation is carried out at 40 MeV. This may be seen in Fig. 3 of paper I. A zero cutoff radius of 0.6 F would seem to avoid the resonant behavior of the $^3P_2$ state and yet preserve the Born character of the pole fit. For further discussion of zero cutoff see paper I, Sec. III.

Zero cutoff appears to provide a satisfactory solution[37,38] to the bound-state problem and we adopt this

form of cutoff in the succeeding calculations. The new potential V' is therefore defined to be

$$V' = \begin{cases} 0, & 0 < r < z_0 \\ V(r), & z_0 < r. \end{cases}$$

z_0 is taken to be 0.6 F. (Incidentally, the symbol "z_0" is adopted to make it explicit that this is a zero-cutoff radius, not a hard core radius. To use a hard core would defeat a major purpose of this work, that being to account for the inner repulsion through the ω field.)

With the one-boson-exchange potentials suitably regularized, the meson parameters are adjusted to provide a fit to the phenomenological phase shifts in a straightforward manner. The six one-boson-exchange potentials described in Sec. III are summed and inserted in the Schrödinger equation. The nuclear bar phase shifts are calculated and compared with graphs of the experimental phase shifts. Adjustments are made in the parameters and further comparisons are made until a reasonable fit to the phase-shift data is secured.

[36] N. Levinson, Kgl. Danske Videnskab. Selskab, Mat. Fys. Medd. 25, No. 9 (1949).

[37] For S states this may not be such a good procedure: Both the $^1S_0$ and the $^3S_1$ phase shifts decrease monotonically with increasing energy. In the case of the $^1S_0$, in fact, the phase shift decreases to $-48°$ at 657 MeV, according to the analysis due to Hoshizaki and Machida (Ref. 38). To provide the repulsion thus evidenced at very short distances, it would be better to impose cutoff in

momentum space. In fitting P states and higher, however, either cutoff should work equally well up to 320 MeV.

[38] N. Hoshizaki and S. Machida, Progr. Theoret. Phys. (Kyoto) 29, 185 (1963).

The six mesons whose one-boson-exchange potentials comprise the net potential are the ω, σ_0, η, ρ, σ_1, and π, as described in Sec. III. The parameters varied are g_ω^2, g_0^2, m_0, g_η^2, f_ρ/g_ρ, g_ρ^2, g_1^2, m_1, and g_π^2. The mass of the ω, η, ρ, and π are taken from experiment, such as summarized in Refs. 24 and 25, and listed in Table II. Note that the mass widths of the particles are neglected. f_ω/g_ω is taken to be zero.

The meson parameters were primarily determined by fitting the P and the D state phase shifts. The F state data only helped fix g_π^2 and m_0. This is because the F states are much less sensitive than the P or D states to the high-mass mesons, and have little weight in the over-all adjustment of the high-mass parameters. Previous experience has shown that a low mass for the σ_0 meson, say 280 MeV, would make the F phase shifts several degrees too positive at 320 MeV, however, so m_0 was fixed at $4m_\pi$. g_π^2 was restricted to the range 11 to 16 to conform with the value of the pion-nucleon coupling constant determined by the higher partial waves in Moravcsik-type modified phase-shift analyses. Various determinations of g_π^2 are listed earlier in this section.

In fitting the P and D phase shifts it developed that $g_\rho^2 R_{12}$ had been overestimated (Sec. III): It turns out that it is more important to match $V_{\sigma\sigma}^{(1)}$ in the middle region than $V_T^{(1)}$ near one F. The remaining parameters came out more or less as expected.

The best set of parameters achieved is listed in Table II. The corresponding phase shifts are tabulated in Table III. (G states are also given for those who may be interested—the phase shifts are given primarily by the pion pole.) The phase shifts are graphed as solid lines in Figs. 6, 7, and 8 where they may be compared with the results of phase-shift analysis. Also, the summed one-boson-exchange potentials corresponding to the Table II parameters are graphed as solid lines in Figs. 2 and 3. There they may be compared with the modified Yale and Hamada-Johnston potentials. Finally, the parameters of Table II are plotted in Figs. 4 and 5 with an "$\times$" so they may be compared with our earlier estimates in Sec. III.

TABLE II. Parameters of the six-meson fit.[a]

Searched parameters.

$g_\eta^2 = 7.0$	$g_\pi^2 = 11.7$
$g_0^2 = 9.4$	$g_1^2 = 6.5$
$m_0 = 560$ MeV	$m_1 = 770$ MeV
$g_\omega^2 = 21.5$	$g_\rho^2 = 0.68$
	$f_\rho/g_\rho = 1.8$

Predetermined parameters.

$m_\eta = 548$ MeV	$m_\pi = 138.2$ MeV
$m_\omega = 782$ MeV	$m_\rho = 760$ MeV
$f_\omega/g_\omega = 0$	

[a] All potentials set equal to zero within 0.6 F.

TABLE III. Nuclear bar phase shifts,[a] in degrees, for parameters of Table II.

E_{lab} (MeV)	$^1P_1$	ϵ_1	$^3P_0$	$^3P_1$	$^3P_2$	$^1D_2$	ϵ_2	$^3D_1$	$^3D_2$	$^3D_3$	$^1F_3$	ϵ_3	$^3F_2$	$^3F_3$	$^3F_4$	$^1G_4$	ϵ_4	$^3G_3$	$^3G_4$	$^3G_5$
10	−2.75	3.96	3.16	−1.79	0.54	0.13	−0.16	−0.49	0.72	−0.00	−0.06	0.07	0.01	−0.02	0.00	0.00	−0.00	−0.00	0.01	−0.00
20	−4.94	5.97	6.30	−3.62	1.55	0.41	−0.50	−1.75	2.27	−0.09	−0.24	0.31	0.05	−0.12	0.01	0.02	−0.02	−0.03	0.08	−0.00
30	−6.58	7.03	8.47	−5.14	2.72	0.71	−0.86	−3.21	4.04	−0.00	−0.49	0.65	0.12	−0.26	0.02	0.05	−0.06	−0.07	0.22	−0.01
40	−7.91	7.66	9.78	−6.44	3.95	1.04	−1.20	−4.64	5.85	0.02	−0.74	1.02	0.20	−0.42	0.05	0.08	−0.11	−0.14	0.40	−0.03
60	−10.11	8.33	10.73	−8.65	6.35	1.74	−1.78	−7.31	9.31	0.15	−1.20	1.76	0.37	−0.75	0.13	0.17	−0.22	−0.32	0.86	−0.07
80	−12.03	8.66	10.29	−10.56	8.49	2.50	−2.21	−9.65	12.42	0.34	−1.60	2.45	0.54	−1.06	0.25	0.25	−0.34	−0.56	1.36	−0.11
100	−13.83	8.83	9.11	−12.29	10.31	3.32	−2.52	−11.71	15.13	0.58	−1.93	3.07	0.69	−1.35	0.40	0.34	−0.46	−0.82	1.89	−0.16
120	−15.57	8.91	7.51	−13.92	11.81	4.19	−2.73	−13.53	17.45	0.83	−2.20	3.61	0.84	−1.62	0.59	0.43	−0.58	−1.10	2.41	−0.21
160	−18.92	8.92	3.73	−16.95	14.02	6.02	−2.92	−16.60	21.03	1.30	−2.64	4.52	1.07	−2.08	1.06	0.60	−0.80	−1.70	3.45	−0.28
200	−22.14	8.78	−0.31	−19.78	15.44	7.88	−2.89	−19.11	23.44	1.64	−2.98	5.23	1.21	−2.48	1.66	0.78	−1.00	−2.31	4.45	−0.32
240	−25.22	8.53	−4.35	−22.44	16.31	9.70	−2.73	−21.21	24.98	1.83	−3.28	5.78	1.24	−2.83	2.37	0.98	−1.18	−2.90	5.41	−0.34
280	−28.16	8.18	−8.27	−24.96	16.82	11.42	−2.47	−22.97	25.87	1.86	−3.57	6.21	1.18	−3.17	3.19	1.20	−1.33	−3.48	6.31	−0.34
320	−30.96	7.73	−12.04	−27.35	17.09	13.02	−2.16	−24.46	26.29	1.75	−3.88	6.55	1.00	−3.50	4.11	1.42	−1.47	−4.03	7.16	−0.31

[a] $T=1$ phase shifts determined by matching Coulomb wave functions asymptotically. $T=0$ phase shifts determined by matching spherical Bessel functions asymptotically.

V. DISCUSSION

A. The Nucleon-Nucleon Predictions

The six-pole fit to the nucleon-nucleon data accounts for the P, D, and F phase shifts fairly well, according to Figs. 6, 7, and 8. Most of our predicted curves fall between or quite close to the experimental values. Since many states are involved we will discuss each in turn.

$^1P_1$: The predicted curve is in agreement with rather widely scattered data.

ϵ_1: Experimentally, the least well determined state. Hull et al.[27] were not even able to determine the sign of ϵ_1 at low energies. Our curve shows the predominant effect of the pion contribution. Note the over-all qualitative agreement with YLAN3M. The monotonic increase in ϵ_1 indicated by the KS points seems in error.

$^3P_0$: The pole-predicted curve agrees well with phase shift analysis except in the range 50 to 100 MeV. Here our curve is consistently below the average experimental value. This is probably due to the lower value of g_π^2 used in this analysis.

$^3P_1$: A reasonably good fit here, but with the predicted curve a degree or two high in the middle energy region.

$^3P_2$: A reasonably good fit here.

$^1D_2$: Agreement here—although the predicted curve may be a degree or two high at 300 MeV.

ϵ_2: Good agreement.

$^3D_1$: Good agreement.

$^3D_2$: Apparently qualitative disagreement here. Our predicted curvature seems too small. Still, the curve straddles YLAN3M and KS at 95 MeV, matches both at 210 MeV, and seems only completely in error at 310 MeV. However, it is not clear that the experimental data are that good at 310 MeV.

$^3D_3$: An interesting case. There is good agreement with KS but not with YLAN3M. It would help to have another phase-shift analysis of the experimental data— as well as more data—at the high end of the energy spectrum.

$^1F_3$: Prediction consistent with rather scattered data points. Note, however, that the F phase shifts are magnified four times with respect to the P or D phase shifts on the ordinate of Fig. 8.

ϵ_3: Experimentally, this phase parameter is not very well determined above 100 MeV. All phase shift analyses except YLAN3M assume pion pole values (indicated by "x"'s inside the symbol). This is probably not correct at high energies. Furthermore, the value of g_π^2 used in the pole fit can vary by as much as 30%. Our curve generally agrees with YLAN3M.

$^3F_2$: Reasonable agreement with somewhat scattered data.

$^3F_3$: Reasonable agreement, only data scattered even more.

$^3F_4$: Fair agreement. Our curve climbs somewhat above the range of experimental values at 300 MeV.

In summing up, it appears that quite a lot of data have been correlated by relatively few parameters. The greatest disagreement occurs in the predictions for the ϵ_1, $^3P_0$, and $^3D_2$ phase parameters. (No attempt has been made to fit the $^1S_0$ and $^3S_1$ states, but it may be reassuring to note that their qualitative behavior— positive at low energy and monotonically decreasing with increasing energy—is nonetheless reproduced. Quantitatively, the $^1S_0$ is found to be too positive and the $^3S_1$ too negative throughout the energy range.)

It may now be of interest to look at the potentials corresponding to the predicted set of meson parameters. These potentials are in surprisingly good agreement with the models of Lassila et al. and Hamada and Johnston for distances greater than 1.2 F. But perhaps this agreement should not be so surprising: Yale and HJ agree, and since our potential predicts about the same $l \geq 1$ phases, it should agree with these too, for the phase shifts are quite sensitive to variations in the potentials beyond 1.2 F, and a single phase-shift solution will bring the several potentials together.

Perhaps the most interesting potential is the isoscalar central potential, $V_C^{(0)}$. Since it results from averaging over the spin and isospin of the two-nucleon potential, it is really the heart of the N-N interaction. Note that the inner repulsion and outer attraction, resulting from the conflicting fields of the ω and the σ_0, provide a simple mechanism for nuclear saturation and average binding. This reminds us of the work of Johnson and Teller,[39] and Duerr,[40] who based nuclear calculations on the idea of counteracting vector and scalar fields.

B. Relation to Other Experiments

Although the meson parameters have been determined just from fitting the nucleon-nucleon data, they, of course, relate to other physical processes as well. Thus, we may make predictions for those experiments involving the same vertices as the N-N system.

Let us first consider the vector meson-nucleon interactions. From Table II, the predicted parameters are seen to be $g_\omega^2 = 21.5$, $g_\rho^2 = 0.68$, and $f_\rho/g_\rho = 1.8$; f_ω/g_ω is implicitly determined to be 0. Note that the ω meson couples more strongly to the nucleon than any other meson considered in this study. However, we have ignored any possible contribution from the ϕ meson, and as it has exactly the same quantum numbers as the ω, there is the strong possibility that some of the interaction strength attributed to the ω is really due to the ϕ. Nevertheless, we do not expect the ϕ to be too important because of its high mass, which will limit its effect on all but S states. A reasonable estimate of isoscalar vector meson effects can be made by requiring that the spin-orbit potential be equal in strength to the phenomenological potential $V_{LS}^{(0)}$ near 1.2 F. Equiva-

[39] M. H. Johnson and E. Teller, Phys. Rev. 98, 783 (1955).
[40] H. Duerr, Phys. Rev. 103, 469 (1956); 109, 117 (1958).

lently, we require that the sum of the spin-orbit potentials due to the ω and the ϕ be equal to the spin-orbit potential produced by the ω alone in the previous work. We have, therefore, that

$$V_{LS}^{(\omega)}(g_\omega^2, 1.2\ F) + V_{LS}^{(\phi)}(g_\phi^2, 1.2\ F)$$
$$= V_{LS}^{(\omega)}(g_\omega^2 = 21.5, 1.2\ F).$$

This equation may be evaluated according to the formulas of Sec. II to yield

$$0.30g_\phi^2 + g_\omega^2 = 21.5. \qquad (5.1)$$

From the above estimate it can be seen that g_ω^2 is not likely to be small even if the ϕ is coupled strongly. For example, if $g_\phi^2 = g_\omega^2$, both coupling constants will be 17.

Our estimate for the ρ-nucleon coupling constant does not seem unreasonable. However, our actual value of g_ρ^2 is lower than expected on the basis of universal ρ coupling to the isospin current, e.g., Sakurai estimates $g_\rho^2 \approx 2$ from ρ decay.[41] Our value of 0.68 may not be all that well determined. In an earlier estimate (which did not fit the phase shifts too badly) we found for the N-N pole parameters

$$g_\rho^2 = 2, \quad f_\rho/g_\rho = 1, \quad g_\omega^2 = 24,$$
$$g_1^2 = 2.75, \quad m_1 = 560\ \text{MeV},$$
$$g_0^2 = 10.25, \quad m_0 = 560\ \text{MeV}, \quad g_\pi^2 = 11, \quad g_\eta^2 = 11.$$

Thus, a value of $g_\rho^2 = 2$ does not seem inconsistent with the N-N pole fit. (Actually the more stable ρ parameter seems to be f_ρ^2, fixed at about 2.)

The vector meson parameters also relate to electron-proton scattering. If the nucleon electromagnetic form factors are assumed to be dominated by the ω, the ϕ, and the ρ, then the isovector form factor data are consistent with our value of $f_\rho/g_\rho = 1.8$, both in sign and in magnitude. The isoscalar parameters are less well known but are consistent with $f_\omega/g_\omega = 0$. (On these points see, e.g., the results of de Vries, Hofstadter, and Herman.[42]) This agreement is very encouraging. It seems to be convincing evidence that it is indeed the ρ and ω (and ϕ) which are responsible both for short-range N-N effects and nucleon electromagnetic structure.

A more specific estimate of the vector meson coupling constants based on the electromagnetic form factor data has been made by Coleman and Schnitzer[43] using their "vector mixing" approximation and the predictions of unitary symmetry. Their estimates for the ϕ and ω (direct) coupling constants seem too large, but agree in order of magnitude with our findings. Their estimate for the ρ-nucleon parameters, on the other hand, are as close to ours as we should expect: Their

values, converted according to our definitions, read $g_\rho^2 = 1.2$ and $f_\rho/g_\rho = 2.1$. [In this connection we remind ourselves that the nonrelativistic approximation invoked in taking the one-boson-exchange potentials brings about the greatest error in the case of the ρ (see Sec. II). Although this should not effect our qualitative conclusions, it makes us wary of percentage comparisons.]

Let us now consider the scalar mesons. Since these mesons have not been established experimentally, their introduction must certainly remain controversial. Perhaps, for example, the σ_0, which decays strongly into two pions, only represents some average effect of a two-pion uncorrelated contribution such as calculated by Amati, Leader, and Vitale[44] or Cottingham and Vinh Mau.[45] There is at least evidence for a strong S-wave $\pi\pi$ interaction, however, so our particle representation may have some basis.

There is, for example, the well-known "ABC" effect: Booth and Abashian have studied the reaction $p + d \rightarrow \text{He}^3 + 2\pi$ and have observed a peaking in the 2π effective mass spectrum near 310 MeV.[46] However, this mass seems to be too low to be consistent with our σ_0 mass of 560 MeV.

Kirz, Schwartz, and Tripp [47] have studied the reaction $\pi^- + p \rightarrow \pi^+ + \pi^- + n$ for several different incident pion energies ranging from 360 to 780 MeV (lab). In the case of the 360-MeV incident beam, they observe a strong peaking in the 2π effective mass spectrum near 400 MeV. They deduce that this effect occurs in the $T = 0$ state because similar peaking fails to appear in the reactions $\pi^- + p \rightarrow \pi^- + \pi^0 + p$, observed by Barish, Kurz, Perez-Mendez, and Solomon,[48] or in the reaction $\pi^+ + p \rightarrow \pi^+ + \pi^+ + n$, observed by themselves.[49] The $T = 0$ effect seems to be different from that of a resonance, however, because as the pion beam energy is increased, the dipion peak shifts over to higher effective mass values—tending toward the kinematic limit—and diminishes in strength. In any case, the peak for low-pion beam energies is observed in other laboratories. Blokhintseva et al.[50] observe the same peak in this reaction using incident pions of 340-MeV energy. Also, in the same reaction but for 240-MeV incident pions,

[41] J. J. Sakurai, in *Proceedings of the International Conference on High-Energy Nuclear Physics, CERN*, edited by J. Prentki (CERN, Geneva, 1962), p. 176.

[42] C. de Vries, R. Hofstadter, and R. Herman, Phys. Rev. Letters 8, 381 (1962).

[43] S. Coleman and H. J. Schnitzer (to be published).

[44] D. Amati, E. Leader, and B. Vitale, Nuovo Cimento 17, 68 (1960); 18, 409, 458 (1960); Phys. Rev. 130, 750 (1963).

[45] W. N. Cottingham and R. Vinh Mau, Phys. Rev. 130, 735 (1963).

[46] N. E. Booth and A. Abashian, Phys. Rev. 132, 2314 (1963), and earlier work cited therein.

[47] J. Kirz, J. Schwartz, and R. D. Tripp, Phys. Rev. 130, 2481 (1963).

[48] R. J. Kurz, B. C. Barish, V. Perez-Mendez, and J. Solomon, Bull. Am. Phys. Soc. 7, 280 (1962), and private communication.

[49] J. Kirz, J. Schwartz, and R. D. Tripp, Phys. Rev. 126, 763 (1962).

[50] T. D. Blokhintseva, V. G. Grebinnik, V. A. Zhukov, G. Libman, L. L. Nemenov, G. I. Selivanov, and Y. Jun-Fang, Zh. Experim. i Teor Fiz. 44, 116 (1963) [English transl.: Soviet Phys.—JETP 17, 80 (1963)].

Batusov et al.[51] observe a displacement in the 2π mass spectrum toward the high-mass values, limited kinematically to a maximum of 350 MeV in this instance.

There is less experimental evidence for a $T=1$, $J=0^+$ meson. This meson will decay strongly into five pions, given sufficient energy. Otherwise it decays into two or four pions violating G parity. S. Zorn[52] has observed a peak in the dipion mass spectrum near 570 MeV in the reaction $p+p \rightarrow d+\pi^++\pi^0$. Lichtenberg[3] has studied this and other data and concluded that the evidence is consistent with the two-pi decay of a $T=1$, $J=0^+$ meson. However, as there have not been confirming experiments for this peak, the meson remains in doubt.

We would like to remark before going on that there is at least one qualitative argument in favor of the $\sigma_{\underline{1}}$. If the bosons are thought to be bound states of the $N-\bar{N}$ system (Fermi-Yang model),[53] then the η and the π are the $T=0$ and $T=1$ $^1S_0$ $N-\bar{N}$ states and the ω and the ρ are the $T=0$ and $T=1$ $^3S_1$ states. The σ_0, if it exists, is the $T=0$ $^3P_0$ bound state. But then there should be a nearby $T=1$ $^3P_0$ level. This will be the σ_1.

Let us now discuss the pseudoscalar meson parameters. g_η^2 is probably not determined too well. Although the present estimate is $g_\eta^2=7.0$ (Table II), g_η^2 was earlier estimated to be ≈ 11 (Sec. III). Perhaps we should not be surprised if later analysis places g_η^2 somewhere between these two estimates.

The pion-nucleon coupling constant has been determined to be 11.7 in this analysis. This is a lower value than is customarily quoted on the basis of pion-nucleon scattering, e.g., Hamilton and Woolcock[54] determine $(m_\pi/2M)^2 g_\pi^2 = 0.081 \pm 0.002$, or, taking the charged pion mass, $g_\pi^2 = 14.7 \pm 0.4$. On the other hand, our value is consistent with g_π^2 as fixed by the $N-N$ higher partial waves in Moravcsik-type phase-shift analyses. Referring to Sec. IV, we observe the following values for g_π^2 for those cases where it is allowed to vary in the search: (1) 11.6 ± 1.2, KS, 147 MeV; (2) 11.8 ± 2.5, PENN, 142 MeV; (3) 13.0, MAD, 142 MeV; (4) 12.8 ± 1.5, KS, 95 MeV; (5) 14.4 ± 0.8, KS, 210 MeV; (6) 16.2 ± 1.3, KS, 310 MeV. In the first two cases cited, the authors chose to redo the analysis with g_π^2 fixed near 14. However, it is not unreasonable that $g_\pi^2 \approx 12$ may be more appropriate to $N-N$ scattering than the higher value.

[51] Y. A. Batusov, S. A. Bunyatov, V. M. Sidorov, and V. A. Yarba, Zh. Eksperim. i Teor. Fiz. 43, 2015 (1962) [English transl.: Soviet Phys.—JETP 16, 1422 (1963)].
[52] B. Sechi Zorn, Phys. Rev. Letters 8, 282 (1962).
[53] E. Fermi and C. N. Yang, Phys. Rev. 76, 1739 (1949).
[54] J. Hamilton and W. S. Woolcock, Rev. Mod. Phys. 35, 737 (1963).